Engineering Hybrid-Hydrogels Comprised of Healthy or Diseased Decellularized Extracellular Matrix to Study Pulmonary Fibrosis

Kamiel S. Saleh,[1] Rukshika Hewawasam,[1] Predrag Šerbedžija,[1] Rachel Blomberg,[1] Saif E. Noreldeen,[1] Benjamin Edelman,[2] Bradford J. Smith,[1,6] David W. H. Riches,[2,3,4,5] and Chelsea M. Magin [1,3,6]

[1]Department of Bioengineering, University of Colorado, Denver | Anschutz Medical Campus, 2115 N Scranton Street, Suite 3010, Aurora, CO 80045, USA; [2]Program in Cell Biology, Department of Pediatrics, National Jewish Health, Denver, CO, USA; [3]Division of Pulmonary Sciences and Critical Care Medicine, Department of Medicine, University of Colorado, Anschutz Medical Campus, Aurora, CO, USA; [4]Department of Research, Veterans Affairs Eastern Colorado Health Care System, Aurora, CO, USA; [5]Department of Immunology and Microbiology, University of Colorado, Anschutz Medical Campus, Aurora, CO, USA; and [6]Department of Pediatrics, University of Colorado, Anschutz Medical Campus, Aurora, CO, USA

Associate Editor Cheng Dong oversaw the review of this article.

Abstract—Idiopathic pulmonary fibrosis is a chronic disease characterized by progressive lung scarring that inhibits gas exchange. Evidence suggests fibroblast-matrix interactions are a prominent driver of disease. However, available preclinical models limit our ability to study these interactions. We present a technique for synthesizing phototunable poly(ethylene glycol) (PEG)-based hybrid-hydrogels comprising healthy or fibrotic decellularized extracellular matrix (dECM) to decouple mechanical properties from composition and elucidate their roles in fibroblast activation. Here, we engineered and characterized phototunable hybrid-hydrogels using molecular techniques such as ninhydrin and Ellman's assays to assess dECM functionalization, and parallel-plate rheology to measure hydrogel mechanical properties. These biomaterials were employed to investigate the activation of fibroblasts from dual-transgenic Col1a1-GFP and αSMA-RFP reporter mice in response to changes in composition and mechanical properties. We show that reacting functionalized dECM from healthy or bleomycin-injured mouse lungs with PEG alpha-methacrylate (αMA) in an off-stoichiometry Michael-addition reaction created soft hydrogels mimicking a healthy lung elastic modulus (4.99 ± 0.98 kPa). Photoinitiated stiffening increased the material modulus to fibrotic values (11.48 ± 1.80 kPa). Percent activation of primary murine fibroblasts expressing Col1a1 and αSMA increased by approximately 40% following dynamic stiffening of both healthy and bleomycin hybrid-hydrogels. There were no significant differences between fibroblast activation on stiffened healthy versus stiffened bleomycin-injured hybrid-hydrogels. Phototunable hybrid-hydrogels provide an important platform for probing cell-matrix interactions and developing a deeper understanding of fibrotic activation in pulmonary fibrosis. Our results suggest that mechanical properties are a more significant contributor to fibroblast activation than biochemical composition within the scope of the hybrid-hydrogel platform evaluated in this study.

Keywords—Hydrogel, Biomaterial, Lung, *In Vitro* model.

Address correspondence to Chelsea M. Magin, Department of Bioengineering, University of Colorado, Denver | Anschutz Medical Campus, 2115 N Scranton Street, Suite 3010, Aurora, CO 80045, USA. Electronic mail: chelsea.magin@cuanschutz.edu
Kamiel S. Saleh and Rukshika Hewawasam have contributed equally to this work.

INTRODUCTION

Idiopathic pulmonary fibrosis (IPF) is a chronic lung disease characterized by excessive proliferation of fibroblasts,[15] pathological extracellular matrix (ECM) deposition and remodeling,[18] increased tissue stiffness, impaired gas exchange, and ultimately respiratory failure.[32,44] Preclinical models of IPF[3,6,34] have been invaluable in uncovering potential drivers of disease progression,[16,22] identifying biomarkers for improved diagnosis,[46] and discovering new therapeutics.[22,38,43,45] Rodents treated with a single dose of bleomycin, for example, display symptoms reminiscent of pulmonary fibrosis, including parenchymal inflammation, epithelial cell injury, increased fibroblast activation and differentiation, and ECM remodeling, which peak two to three weeks after injury.[9] Time-resolved analysis of the lung proteome revealed that 154 matrisome proteins were significantly changed after administration of bleomycin, indicating substantial biochemical changes

accompany the biomechanical alterations, i.e., tissue stiffening observed in fibrotic lung injury.[37] This combination of altered ECM composition and mechanics has been indicated as a key driver of pathological gene expression in fibroblasts.[12,14,28] However, less is known about how composition and mechanics independently regulate fibroblast activation. Here, we present a strategy for engineering hybrid-hydrogels with a phototunable poly(ethylene glycol) backbone containing healthy or bleomycin-injured (fibrotic) murine decellularized ECM (dECM) in a way that decouples biochemical composition from mechanics to study fibroblast-matrix interactions *in vitro*.

Techniques in lung decellularization have gained traction alongside a growing interest in accurately modeling the composition and mechanical properties of the extracellular environment of fibrotic lung tissue.[4,7] For example, Booth *et al.* measured the Young's modulus of healthy and IPF human lungs before and after decellularization. Prior to decellularization the elastic modulus of healthy lung tissue was measured to be 1.96 ± 0.13 kPa with a wide range of values reported from 0.5 up to 9 kPa. Fibrotic lung tissue prior to decellularization exhibited an elastic modulus that was significantly higher 16.52 ± 2.25 kPa with an even wider range of measurement values (0.5 to ~ 100 kPa).[5] These results corresponded to many previous studies, which report elastic moduli ranges as healthy (1–5 kPa) and fibrotic (> 10 kPa) with significant heterogeneity.[8,19,21] Following decellularization, the elastic modulus of both healthy and IPF lungs decreased as did the difference between the two.[5] Using decellularized precision-cut lung slices, Parker *et al.* showed that diseased ECM, not fibroblasts from IPF lungs, was the primary modulator of pathologic gene expression.[28] Several studies have generated dECM-derived hydrogels to preserve the complex biochemical milieu of native tissue.[8,30,35] For instance, de Hilster *et al.* developed dECM hydrogels from control and diseased human lungs that replicated trends in mechanical properties, e.g., increased stiffness for IPF-derived dECM hydrogels, but did not fully reproduce the values of mechanical properties measured for healthy or diseased lung tissue.[8] Several strategies have been employed to overcome this limitation, including photoinitated crosslinking of dECM proteins,[27] coating of poly(acrylamide) hydrogels with varying elastic modulus values with healthy and diseased dECM,[36] and even incorporating dECM into hybrid-hydrogels that enable user-controlled stiffening of the cellular microenvironment.[29]

User-controlled dynamic stiffening has been achieved through a variety of dual-stage polymerization hydrogel systems.[1] Dual-stage polymerization of-ten proceeds *via* a click reaction mechanism, such as a thiol-Michael addition. This reaction occurs with high specificity under mild reaction conditions and is followed by a user-controlled mechanism, such as a photoinitiated secondary reaction to manipulate hydrogel mechanics. For example, Gillette *et al.* employed a collagen-alginate composite hydrogel to increase or decrease stiffness of the microenvironment when divalent cations were added to or removed from the system, respectively.[11] Furthermore, Rosales *et al.* developed a dual-polymerization system capable of dynamically switching hydrogel modulus values through a combination of photopolymerization and photodegradation.[33] More recently, Petrou *et al.* engineered a hybrid-hydrogel dual-stage polymerization model that combined a phototunable poly(ethylene glycol)-alpha methacrylate (PEGαMA) synthetic backbone with porcine lung dECM, demonstrating that dynamically stiffening the hydrogel resulted in significant increases in fibroblast activation.[29]

Here, we build on this work by presenting a strategy that incorporates both healthy and bleomycin-injured (fibrotic) dECM within a dual-stage photopolymerization system. This new hydrogel offers precise control of both the mechanical properties and biochemical composition of the cellular microenvironment. To accomplish this, healthy and bleomycin-treated murine pulmonary tissue were decellularized following established guidelines[7] and dECM solubility and free-amine content were tailored for incorporation into hybrid-hydrogels. Hydrogel formulations reproducibly replicated elastic moduli of healthy and fibrotic tissues, before and after stiffening respectively. Evaluation of fibroblasts cultured on these surfaces revealed that matrix stiffness was a more significant contributor to activation to the myofibroblast phenotype as measured by alpha-smooth muscle actin (αSMA) and collagen 1a1 (Col 1a1) expression than dECM composition. This new biomaterial system will enable future studies of cell-matrix interactions in pulmonary fibrosis and improve our ability to understand, prevent, and treat IPF.

METHODS

PEGαMA Synthesis and Characterization

PEGαMA was synthesized as previously described.[29] Briefly, poly(ethylene glycol)-hydroxyl (PEG-OH; 8-arm; 10 kg mol^{-1}; JenKem Technology) was lyophilized. Next, PEG-OH (5 g, 0.004 mol of hydroxyls) was dissolved in anhydrous tetrahydrofuran (THF; Sigma) in a flame-dried Schlenk flask under

moisture-free conditions. Anhydrous sodium hydride (0.38 g, 0.015 mol) was added to the flask and reacted with PEG-OH at room temperature for 45 min. Ethyl 2-(bromomethyl)acrylate (3.68 mL, 0.026 mol) (EBrMA; Ambeed, Inc.) was injected dropwise into the Schlenk flask and the reaction proceeded in a light-protected environment for 48 h. The reaction was neutralized with 1 N acetic acid and filtered through Celite 545 soaked with THF in a medium glass-fritted funnel. The filtrate was concentrated with rotary evaporation at 45 °C and precipitated into diethyl ether (Sigma Aldrich) overnight at 4 °C. The resulting polymer was dialyzed (1 kg mol^{-1} MWCO, Repligen) against 3.5 L of deionized water with a total of four changes over 72 h at room temperature and lyophilized to obtain a white solid product (yield: 64%). PEGαMA functionalization and purity were verified using ^{1}H NMR. ^{1}H NMR spectrum was recorded on a Bruker DPX-400 FT NMR spectrometer (300 MHz). Chemical shifts for protons (^{1}H) were recorded in parts per million (ppm) relative to a residual solvent. ^{1}H NMR (300 MHz, CDCl$_3$): δ (ppm) 1.36 (t, 3H, CH$_3$–), 3.71 (s, 114H, PEG CH$_2$–CH$_2$), 4.29 (t, s, 4H, –CH$_2$–C(O)–O–O, –O–CH$_2$–C($=$CH$_2$)–), 5.93 (q, 1H, –C$=$CH$_2$), 6.34 (q, 1H, –C$=$CH$_2$). End group functionalization of the final PEGαMA polymer was greater than 96% (Fig. S1). Only PEGαMA with functionalization over 95% by comparison of the αMA vinyl end group to the PEG backbone was used in subsequent experiments.

Bleomycin Injury Model

All animal procedures were performed in an AAA-LAC-accredited facility in accordance with the Guide for the Care and Use of Laboratory Animals[26] and approved by the University of Colorado Denver Institutional Animal Care and Use Committee. Dual-transgenic reporter mice (C57BL/6J.αSMA-RFP.Col1a1-GFP) aged 8–12 weeks, male and female, were bred for this study from single-transgenic reporter parents. Fibroblasts from this strain express green fluorescent protein (GFP) under control of the promoter Col1a1 and red fluorescent protein (RFP) under control of the promoter αSMA. Wildtype littermates were used for experiments that did not require reporter cells, such as collection of healthy lungs for decellularization.

Bleomycin (MWI Veterinary Supply) was administered intratracheally to male and female C57BL/6J mice aged 8–9 weeks to initiate development of pulmonary fibrosis.[25,31] Mice were anesthetized with 3% isoflurane and instilled with 3 U kg^{-1} bleomycin in 50 μL phosphate-buffered saline (PBS; Cytiva) directly into the trachea.[25] Mice were maintained for 21 days post-bleomycin administration before harvest, as described below.

Lung Function Assessment

Lung function at 21-days post-bleomycin administration was assessed as previously described.[40] Briefly, mice were anesthetized with ketamine/xylazine/ace-promazine (100/8/2.5 mg kg^{-1}), the trachea was cannulated with a blunted 18-gauge thin-walled needle, and the cannula was attached to a flexiVent FX small animal ventilator (SCIREQ, Montreal, PQ, Canada). Mice were then administered pancuronium bromide (0.8 mg kg^{-1}) to induce paralysis and prevent spontaneous breathing efforts. After a 10 min equilibration period (tidal volume (Vt) = 10 mL kg^{-1}, positive end expiratory pressure (PEEP) = 3 cmH$_2$O, and respiratory rate (RR) = 150 breaths min^{-1}) a lung function assessment was conducted. First, a recruitment maneuver was applied and a stepwise pressure-volume loop was recorded to determine quasi-static compliance (Cst, the slope of the quasi-static points at 5 cmH$_2$O on the expiratory limb) and inspiratory capacity (IC, the volume delivered from 0 to 30 cmH$_2$O). Multi-frequency forced oscillation measurements were then conducted at PEEP = 9, 6, 3, and 0 cmH$_2$O. At each PEEP, a recruitment maneuver was applied and then four 3 s forced oscillations were recorded at 10 s intervals. We report the average elastance (H), calculated by fitting the constant phase model to impedance spectra, for each PEEP. Finally, a 7 min period of ventilation at PEEP = 0 cmH$_2$O was recorded to assess alveolar stability (derecruitment), followed by a 2nd stepwise PV loop. Forced oscillation data are shown in the supplement (Fig. S1).

Murine Lung Decellularization

Murine lungs were harvested from healthy (between 8 and 12 weeks of age) or bleomycin-injured (between 11 and 15 weeks of age) male and female mice and decellularized using a previously established protocol.[4] Briefly, animals were euthanized via CO$_2$ overdose and a cannula was inserted into the trachea. Pulmonary vasculature was cleared of blood by injection of PBS into the right ventricle. The cannulated heart-lung block was excised from the thoracic cavity and sequentially perfused through both the trachea and the right ventricle with a series of solutions and incubation periods: Triton X-100 (0.1%; 6 mL; Fisher BioReagents) for 24 h at 4 °C, sodium deoxycholate (SDC; 2%; 6 mL; Fisher BioReagents) for 24 h at 4 °C, sodium chloride (1 N; 6 mL; Chem Impex) for 1 h at room temperature, and DNase (12 U mL^{-1}; 6 mL; Epicentre) for 1 h at room temperature. Each perfusion and incubation step was followed by a wash step with deionized water (DI water; 20 mL; 100 U mL^{-1} penicillin; 100 μg mL^{-1} streptomycin).

Confirmation of Decellularization

Tissue decellularization was confirmed through nuclear staining and DNA quantification. One decellularized scaffold was used for nuclear assessment and three were used for DNA extraction. A PBS-perfused lung was used as a non-decellularized control in all experiments. Completeness of decellularization was assessed by staining for cell nuclei with 4′,6-diamidino-2-phenylindole (DAPI), visualization of DNA depletion on an agarose gel, and quantification of residual dsDNA. DNA was extracted from three decellularized scaffolds and one non-decellularized control lung tissue using a tissue DNA extraction kit (QIAGEN). The total concentration of remaining DNA in decellularized scaffolds was quantified using a Quant-iT Pico-Green dsDNA Assay Kit (ThermoFisher) according to the manufacturer's instructions. Additionally, equivalent amounts of tissue dry weight (in mg) were dissolved in 100 μL of PBS and loaded as 30 μL samples per lane onto a 0.8% agarose gel containing Gel Red (Biotium). The gel was run for approximately 75 min at 110 V in a tris borate buffer to assess the size of remaining DNA fragments.

Mechanical and Enzymatic Digestion of dECM

Following decellularization, lung lobes were dissected from the heart-lung block, homogenized in 10 mL DI water (gentleMACS Dissociator, Miltenyi Biotec, Inc.), and lyophilized. Total time required for enzymatic digestion of healthy and bleomycin-injured dECM was determined by exposing dECM to pepsin (320 U mg^{-1} tissue; Sigma) in 0.1 N HCl (pH adjusted to 1.5) for 0, 4, 12, 24, and 36 h, followed by neutralization with 0.1 N NaOH.[23] Digested dECM was centrifuged (3500 rpm, 10 min; Sorvall Legend Micro 17 Microcentrifuge, Thermo Scientific) and the supernatant fluid was ultrasonicated (5 min; 100% amplitude; 10 s frequency; Fisherbrand™ Model 705 Sonic Dismembrator) before being flash-frozen for lyophilization.

Lyophilized samples from each time point were evaluated for protein content, amine content, and protein molecular weight distribution. Protein content was measured using a bicinchoninic acid assay (Pierce BCA Protein Assay Kit, Thermo Scientific) following manufacturer's instructions. Amine content was evaluated *via* ninhydin assay (Sigma-Aldrich) following the manufacturer's protocol. Protein molecular weight distribution was quantified using a QuickStain Protein Labeling Kit (Amersham) to evaluate samples run using SDS-PAGE electrophoresis on 4–20% Mini-PROTEAN TGX Precast Protein Gels for approximately 120 min at 100 V in a tris borate buffer, per the

manufacturer's protocol. All subsequent experiments were performed using dECM digested for 36 h as described above.

dECM Functionalization and Characterization

As previously described, dECM was functionalized by converting free amines to thiol that can participate in a thiol-ene Michael addition reaction with PEGαMA.[29] Briefly, Traut's reagent (2-iminothiolane hydrochloride, Sigma) was dissolved at 3 mg mL^{-1} in PBS with 3 mM ethylenediaminetetraacetic acid (EDTA, Sigma). dECM samples were dissolved in Traut's reagent solution and incubated for 1 h at room temperature. The molar excess of Traut's reagent required to minimize amine content following thiolation was identified by measuring amine content at 5, 10, 25, 50, 75 and 100 molar excess Traut's reagent. Thiolated dECM was purified by dialysis (100–500 g mol^{-1} MWCO, Repligen) and lyophilized to obtain pure thiolated dECM. Thiolation was confirmed with ninhydrin and Ellman's assay (Sigma-Aldrich) performed according to the manufacturer's protocol. Based on the results of these analyses, 75 molar excess Traut's reagent was selected for subsequent dECM thiolation.

Hydrogel Synthesis

PEGαMA was reacted with the crosslinkers 1,4-dithiothretiol (DTT; Sigma-Aldrich) and thiolated dECM in a base-catalyzed thiol-ene Michael addition reaction at a 3:8 thiol to αMA off-stoichiometric ratio, which was maintained by using the thiol concentrations measured through Ellman's assays in the hydrogel formulation calculations. The hydrogel formulation was determined by varying the molar ratio (mol%) between healthy murine dECM and DTT to achieve the desired elastic modulus. First, dECM (0.5 mg μL^{-1}) was reacted with 250 mM Tris(2-carboxyethyl)phosphine (TCEP, Sigma) (40 molar excess to thiol groups on the dECM as measured by Ellman's assay) for 45 min at room temperature to obtain the maximum thiolation. Stock solutions of DTT (250 mM), CGRGDS peptide (75 mM), and PEGαMA (0.4 mg μL^{-1}) were prepared in 0.3 M, pH 8 4-(2-hydroxyethyl)-1piperazineethanesulfonic acid buffering agent (HEPES; Life Technologies). Precursor solution consisting of dECM, DTT, CGRGDS (2 mM), and then 18.5 wt% of PEGαMA was added. A 40-μL drop of hydrogel precursor solution was placed between two hydrophobic parafilm-covered glass slides and allowed to polymerize for 45 min at 37 °C for rheology experiments. Hydrogels were equilibrated in PBS overnight with phenyl-2,4,6-trimethylbenzoylphosphi-

nate photoinitiator (LAP; 2.2 mM; Sigma-Aldrich). After equilibration, hydrogels were exposed to 365 nm ultraviolet light at 10 mW cm^{-2} for 5 min to initiate secondary homopolymerization of remaining excess αMA moieties (Lumen Dynamics OmniCure Series 2000 UV lamp). For cell activation experiments, 40 μL of hydrogel precursor was placed between a Sigma-cote-treated glass microscopy slide and a silanated cover slip [(3-aminopropyl)-trimethoxysilane; 12 mm]. Hydrogels polymerized *via* thiol-ene Micheal addition at 37 °C for 45 min. All cell activation experiments were carried out under aseptic conditions. 2D Hybrid-hydrogel samples were then placed in 24-well non-tissue culture treated plates (Greiner BioOne) and equilibrated in sterile PBS overnight prior to experiments. Secondary homopolymerization of excess αMA functional groups was initiated by exposing hydrogels to UV light, stiffening hydrogels for fibrotic activation experiments.

Hybrid-Hydrogel Characterization

Mechanics of the hydrogels were evaluated *via* rheology, following initial thiol-ene Michael addition polymerization and a secondary homopolymerization of αMA groups. Hydrogels (height = 300 μm; diameter = 8 mm) were mechanically tested using a Discovery HR2 rheometer (TA Instruments) with an 8 mm parallel plate geometry. The geometry was lowered until the rheometer registered a 0.03 N axial force. Storage modulus (G') plateau was determined by measuring storage modulus under hydrogel compression in increments of 10% compression.[24] Hydrogel samples underwent a frequency oscillation with logarithmic sweep of frequencies between 1 and 100 rad s^{-1} at 1% strain. Elastic modulus (E) was calculated by assuming that hydrogels exhibited incompressible bulk-elastic characteristics with Poisson's ratio of 0.5.[29]

Primary Cell Isolation

Fibroblasts were isolated from lungs of dual-transgenic reporter mice (C57BL/6J.αSMA-RFP.Col1a1-GFP) aged 8–12 weeks old, both male and female. Following euthanasia, the right ventricle was perfused with PBS and then 1 mL of enzyme solution (5 U mL^{-1} dispase and 2 mg mL^{-1} collagenase 1 in PBS; Life Technologies) was instilled into the lungs through the trachea. Next, lungs were inflated with 0.3 mL warm low melting point agarose (LMP Ultra-pure; Life Technologies) through the trachea. The heart-lung block was placed under ice until the agarose solidified. The heart-lung block was excised, individual lobes were dissected away from the heart and trachea, and

transferred into the same enzyme solution in a gentleMACS C tube (Miltenyi Biotec, Inc). Lung lobes were incubated for 20 min at 37° with rotation before dissociation using a gentleMACS Dissociator (Miltenyi Biotec, Inc.) at 275 rpm for 37 s followed by 3300 rpm for 38 s. The enzymatically and mechanically dispersed lung tissue was sequentially filtered through 70-micron and 40-micron cell strainers. Cells were counted and re-suspended in a buffer containing 0.5% bovine serum albumin (BSA; Sigma) and 2 mM EDTA in PBS (PEB buffer). For every 10^7 cells, 10 μL each of magnetic microbeads conjugated to anti-mouse CD31 (Miltenyi Biotec, Inc.; CD31 MicroBeads; mouse; Catalog Number: 130-097-418) and CD45 (Miltenyi Biotec, Inc.; CD45 MicroBeads; mouse; Catalog Number: 130-052-301) were added to the cell suspension, incubated at 4 °C for 15 min, and passed through LS magnetic columns (Miltenyi Biotec, Inc.) in a Quadromacs Separator (Miltenyi Biotec, Inc.) to exclude CD31$^+$/CD45$^+$ cell populations. Positive selection for fibroblasts was performed with magnetic microbeads conjugated to anti-mouse CD140a (PDGFRα) (Miltenyi Biotec, Inc.; CD140a (PDGFRα) MicroBead Kit; mouse; Catalog Number: 130-101-502) using the same columns.

Fibroblast Activation

PDGFRα+ fibroblasts from dual-reporter (C57BL/6J.αSMA-RFP.Col1a1-GFP) mice (8–12 weeks old) were cultured on 2D hybrid-hydrogels ($N = 6$) to evaluate fibroblast activation. Cells were seeded directly onto soft hydrogels at 20,000 cells cm^{-2} following isolation and cultured in growth medium (DMEM/F12 with 100 U mL^{-1} penicillin, 100 U mL^{-1} streptomycin, 2.5 μg mL^{-1} amphotericin B, and 10% FBS) at 37 °C; 5% CO$_2$. The next day medium was changed to experimental medium (DMEM/F12 with 100 U mL^{-1} penicillin, 100 U mL^{-1} streptomycin, 2.5 μg mL^{-1} amphotericin B, and 1% FBS). On day 6 following cell seeding, cell culture medium was replaced on half of the soft hydrogel samples with medium containing 2.2 mM LAP photoinitiator. The next day (day 7), the soft hydrogels treated with LAP were stiffened by exposure to ultraviolet light (365 nm at 10 mW cm^{-2}) for 5 min. Samples were rinsed to remove residual photoinitiator and incubated in complete medium for two additional days. All samples were collected for analysis on day 9 of culture and processed at room temperature. Samples were rinsed with PBS and fixed with 4% v/v paraformaldehyde (Electron Microscopy Sciences) in PBS for 20 min. After fixation, samples were rinsed with 100 mM glycine (Sigma) in PBS for 15 min. Nuclei were stained with Hoechst (1:200 dilution in deionized water; Sig-

ma) for 15 min. Samples were washed with deionized water and mounted with Prolong Gold Antifade (ThermoFisher).

Microscopy was performed on an upright epifluo-rescent microscope (BX-63; Olympus). Six fields of view were randomly selected and imaged on each sample at ×20 magnification, at constant exposure time between groups. Image analysis was performed by counting cells positive for Col1a1-GFP and/or αSMA-RFP and normalizing to the total number of cells by counting DAPI-positive nuclei. The proportion of cells positive for each reporter was documented.

Fluorescence Microscopy and Image Analysis

Fluorescence microscopy was performed using an upright, epifluorescent microscope (BX-63, Olympus). Six fields of view were randomly selected and imaged on each sample at ×20 magnification maintaining the same imaging settings, including exposure time across all samples. Image analysis for activation experiments was performed using ImageJ software (NIH) to count cells positive for GFP-Col1a1 and/or RFP-αSMA. These cell counts were divided by the total cell number acquired by counting DAPI-positive nuclei to calculate the proportion of GFP-Col1a1-positive and RFP-αSMA-positive cells on each sample.

ImageJ software was also used to quantify total fluorescence intensity of GFP-Col1a1 and/or RFP-αSMA positive fibroblasts, per field of view. Grayscale intensity of each image was recorded using the Mea-sure function. The intensity of each individual image was divided by total cell count for that field of view. These values were averaged to calculate the mean average intensity per cell for each sample type. Finally, the mean intensity for each sample type was normal-ized to the mean intensity for the healthy, soft samples.

Statistics

All quantitative decellularization confirmation and hydrogel characterization experiments were performed with a minimum of $N = 3$ technical replicates. Hydrogel characterization experiments and in vitro experiments were represented by a minimum of $N = 4$ biological replicates. All dECM material was sourced from populations containing equal numbers of male and female mice. Lungs from at least four mice were pooled for each dECM replicate. Unless otherwise stated, data were presented as mean ± standard error of the mean (SEM). GraphPad Prism 9 Software was used to perform all graphing and statistical analyses. Two-way analysis of variance (ANOVA) with Tukey's post hoc multiple comparison tests was performed on each measure with multiple groups being compared

over time. A 2-tailed Student's t-test was used when comparing fewer than three groups where the data followed normal distribution and featured equal vari-ance. Elastance measurements from the lung function assessment did not meet these criteria, so a Welch's t-test was performed on data with unequal variance between groups (PEEP 9) and a Mann–Whitney test on data with a non-normal distribution (PEEP 0, 3, 6). p values of < 0.05 were considered significant.

RESULTS

Bleomycin Injury Model and Murine Lung Decellularization

In this work, we report a strategy for incorporating healthy and bleomycin-injured murine dECM into a phototunable hydrogel system for investigating cellular responses to mechanical and biochemical changes to the microenvironment. Healthy and bleomycin-injured mouse lungs were decellularized, homogenized, di-gested, and lyophilized (Fig. 1a). Lung function mea-surements confirmed bleomycin-induced fibrosis as measured by decreases in both inspiratory capacity (from 0.90 ± 0.05 to 0.62 ± 0.09 mL; Fig. 1b) and quasi-static compliance (from 0.08 ± 0.01 to 0.05 ± 0.01 mL cmH$_2$O^{-1}; Fig. 1c), indicating that bleomycin-treated mice exhibited smaller and stiffer lungs. In support of this, lung elastance (stiffness) measured with forced oscillations was increased at high PEEP (Fig. S3) where the connective tissue network plays the strongest role.[10,17,23] Next, decellularization for both healthy and bleomycin-injured lungs was confirmed by staining for cell nuclei (Fig. 1d), measuring the con-centration of remaining DNA (Fig. 1e), and evaluating the size of remaining DNA fragments (Fig. S2). The lack of cell nuclei observed through DAPI staining and fluorescent microscopy, total average dsDNA con-centrations below 50 ng mg^{-1} for both healthy (16.23 ± 2.28 ng mg^{-1}) and bleomycin-injured (25.49 ± 5.32 ng mg^{-1}) lungs, and no detectable bands for DNA fragments in the size range of 100–25,000 base pairs all indicated complete decellularization according to guidelines established by Crapo et al.[7]

Enzymatic Digestion of dECM

Digestion of dECM from healthy and bleomycin-injured murine lungs was monitored over time by measuring total soluble protein concentration, total free amine concentration, and protein fragment size. The total protein concentration quantified by BCA protein assay of both healthy and bleomycin-injured lung dECM increased between initial measurements
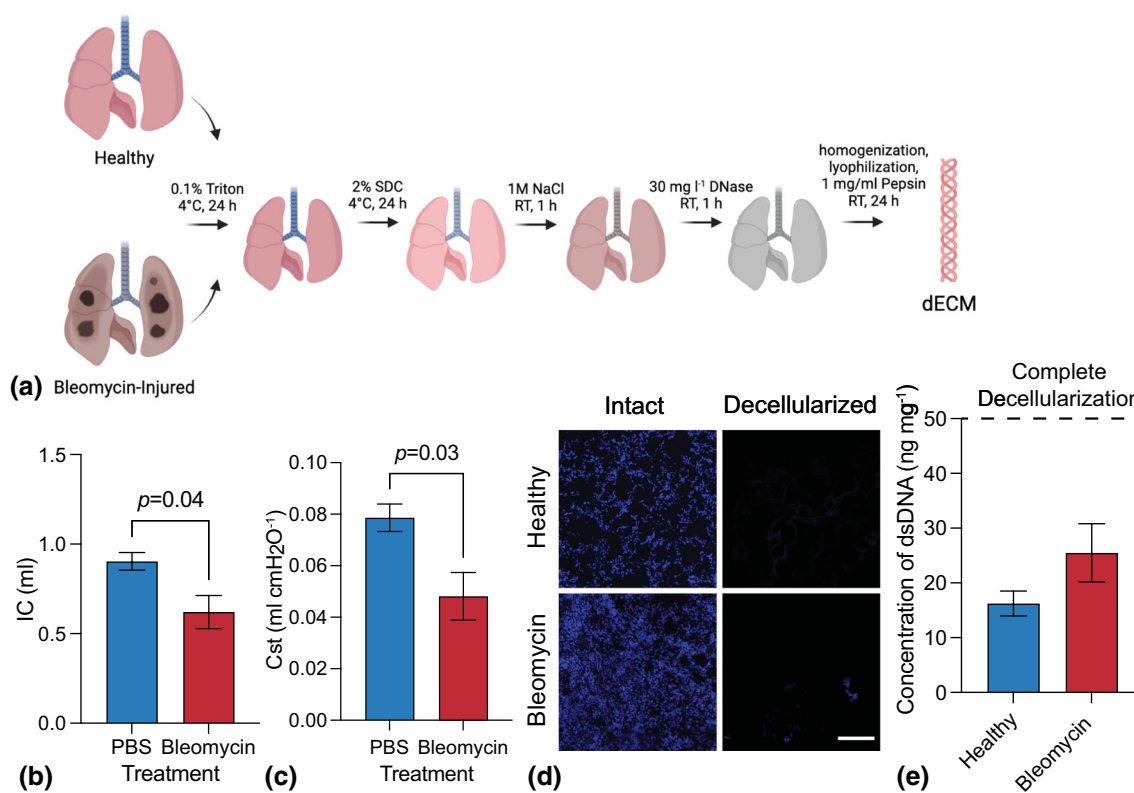
FIGURE 1. (a) Schematic representing the lung decellularization process for both healthy and bleomycin-injured lungs. Lungs were sequentially perfused with detergents, salts, and enzymes before being enzymatically digested and lyophilized. (b) A significant decrease in (b) inspiratory capacity and (c) quasi-static compliance was measured in bleomycin-injured lungs versus controls, indicating reduced air volume in lung due to fibrotic tissue accumulation (N = 5–8; Student's t-test). (d) Representative fluorescent microscopy images of cell nuclei (blue; DAPI) before and after decellularization showed nearly complete removal of cells in healthy and bleomycin-injured mouse lung samples (N = 3, Scale bar 200 μm). (e) Quantification of dsDNA concentration demonstrated decellularized scaffolds containing average dsDNA amounts that were significantly below the threshold for complete decellularization (N = 3).

and 4 h of pepsin digestion, then remained near approximately 660 μg mL^{-1} for healthy and 800 μg mL^{-1} for bleomycin-injured for all subsequent time points (Fig. 2a). These results indicate that 4 h pepsin digestion was sufficient to solubilize dECM proteins. Total free amine concentration, an indicator of how many peptide bonds have been cleaved by pepsin over time, showed an increasing trend from 0.35 to 0.45 μmol mg^{-1} for healthy and 0.32 to 0.39 μmol mg^{-1} for bleomycin-injured over 36 h (Fig. 2b). There was a statistically significant difference ($p < 0.05$) between free amine concentrations measured at 24 and 36 h. These data demonstrate that peptide bond cleavage occurred throughout the digestion process. Qualitative evaluation of protein fragment sizes showed that soluble protein was initially undetectable due to the low solubility of undigested dECM. Prominent bands appeared between 50 and 75 kDa and near 25 kDa for both healthy (Fig. 2c) and bleomycin-injured (Fig. 2d) dECM after 4 h treatment with pepsin. These bands remained visible but decreased slightly in intensity between 12 and 36 h in healthy. In bleomycin, band

intensity for all lanes peaked at 24 h and decreased slightly at 36 h. Taken together with the results from total free amine concentration measurements, these results indicated that even though cleavage of peptide bonds continued over 36 h, there were still relatively large protein fragments present in the soluble fraction of the dECM solution for functionalization and incorporation into hybrid-hydrogels.

dECM Functionalization and Characterization

dECM was functionalized to transform it into a crosslinker capable of undergoing a thiol-ene Michael addition reaction. Naturally occurring free primary amines on the dECM were converted into thiols using Traut's reagent. First, healthy and bleomycin-injured murine dECM samples were treated with 5–100 molar excess Traut's reagent to identify the amount of reagent required to fully convert primary amines to thiols. The average concentration of primary amines as measured by ninhydrin assay decreased for both healthy and bleomycin-injured samples as the molar
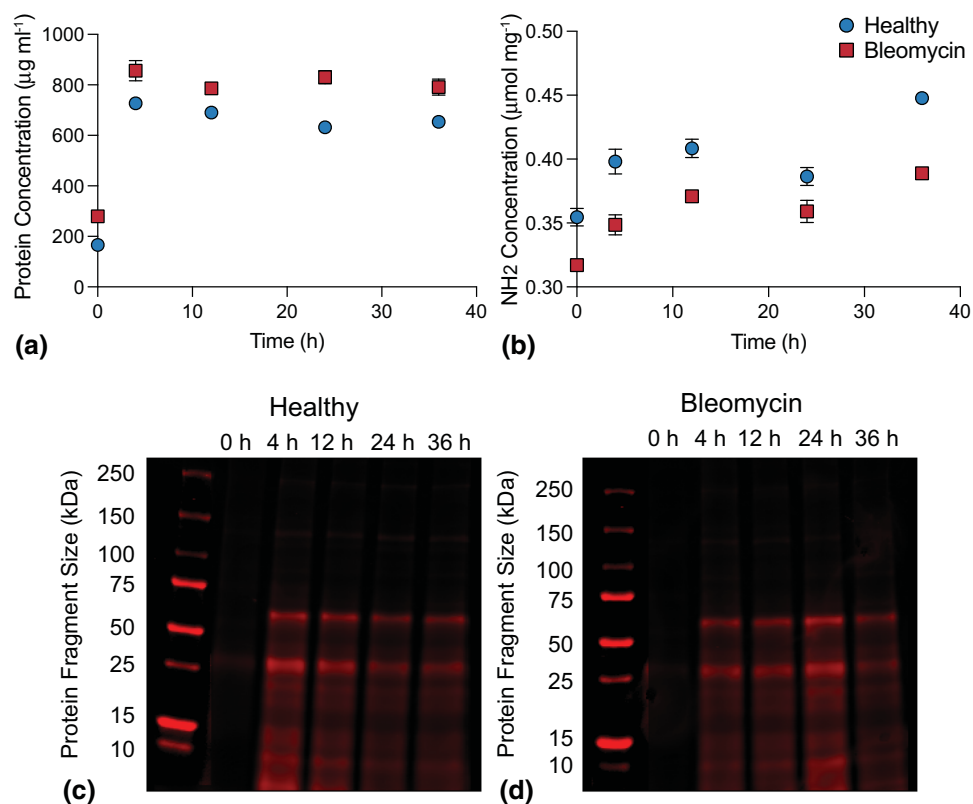
FIGURE 2. (a) Total soluble protein concentration measured in the supernatant of healthy and bleomycin-injured murine lung dECM samples during pepsin digestion over time. Total protein concentration increased from initial measurement to 4 h then plateaued ($N = 4$, ANOVA, Tukey Test). (b) quantification of free amine concentration over time showed that peptide bond cleavage increased with pepsin digestion time ($N = 4$, ANOVA, Tukey Test). Protein fragment size quantification for both (c) healthy and (d) bleomycin-injured murine lung dECM showed pepsin digestion was required to solubilize dECM proteins to fragments ranging in size from 10 to 75 kDa. Despite decreases in band intensity over time for healthy (4–36 h) and bleomycin-treated (24–26 h) qualitative results showed large protein fragments were solubilized for functionalization and incorporation into hybrid-hydrogels ($N = 4$).

excess of Traut's reagent increased and plateaued at 75 molar excess (Fig. 3a). Average primary amine concentrations of healthy (0.40 ± 0.03 μmol mg^{-1}) and bleomycin-injured (0.27 ± 0.01 μmol mg^{-1}) dECM decreased significantly following treatment with Traut's reagent to 0.02 ± 0.004 μmol mg^{-1} and 0.01 ± 0.001 μmol mg^{-1}, respectively. Following reaction with Traut's reagent, thiol concentrations increased significantly from 0.007 ± 0.001 to 0.278 ± 0.002 μmol mg^{-1} for healthy and from 0.006 ± 0.001 to 0.177 ± 0.001 μmol mg^{-1} for bleomycin-injured ($p < 0.0001$, Tukey Test), indicating successful conversion of dECM amines to thiols (Fig. 3b).

Hybrid-Hydrogel Synthesis and Characterization

Hybrid-hydrogels containing either healthy or bleomycin-injured (fibrotic) dECM within a dual-stage photopolymerization system were designed to reproduce the mechanical properties of healthy and fibrotic lung tissue. First, an off-stoichiometry (3:8 thiols to -enes), base-catalyzed Michael addition reaction

between DTT or thiolated dECM and αMA end groups produced a soft hydrogel. Then stiffening was accomplished *via* a homopolymerization of PEGαMA in the presence of LAP photoinitiator and 365 nm UV light (Fig. 4a). Functionalized dECM from healthy lung tissue was crosslinked with 18.5 wt% PEGαMA *via* base-catalyzed thiol-ene Michael addition at various dECM to DTT molar ratios to select a hydrogel formulation exhibiting elastic modulus values for both soft and stiffened in ranges that corresponded to healthy (1–5 kPa) and fibrotic lung tissue (> 10 kPa) (Fig. 4b).[8,19,21] Elastic moduli decreased with increased dECM content. Hydrogels containing 5% and 10% dECM exhibited initial elastic modulus values above 10 kPa, while the 20% and 25% dECM formulations displayed stiffened modulus values below 5 kPa. Only the 15% dECM hydrogel formulations displayed a soft modulus of 5.1 ± 0.59 kPa replicating healthy pulmonary tissues and stiffened modulus of 10.6 ± 0.78 kPa recapitulating fibrotic tissue. Hybrid-hydrogels fabricated with functionalized dECM from bleomycin-injured pulmonary tissue were crosslinked with 18.5
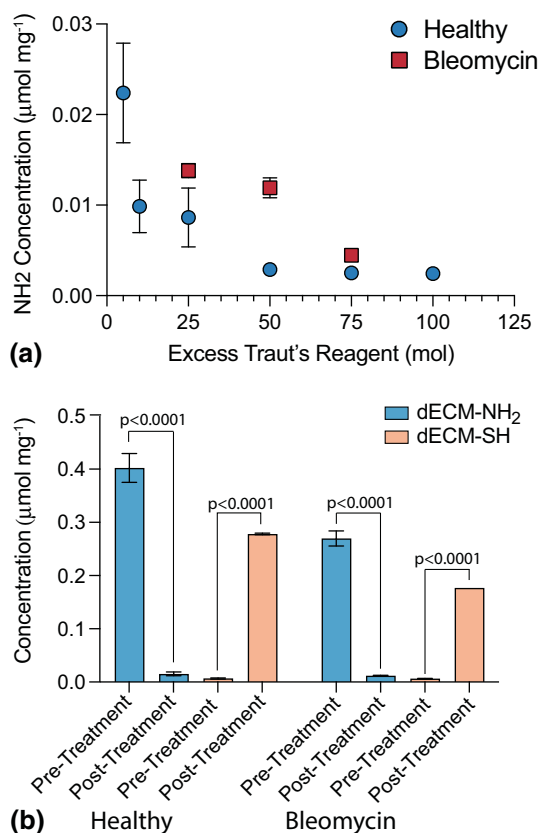
FIGURE 3. (a) Healthy and bleomycin-injured murine lung dECM was treated with excess Traut's reagent ranging from 5 to 100 molar excess to identify the quantity required to completely convert primary amines to thiols, i.e., significantly reduce primary amine content following thiolation (N = 12). Reduction in primary amine content plateaued at 75 molar excess. (b) Amine and thiol content of healthy and bleomycin-injured murine lung dECM was evaluated before and after thiolation *via* ninhydrin and Ellman's assay, respectively (N = 12, ANOVA, Tukey Test). Statistically significant decreases in primary amine concentration and corresponding increases in thiol concentrations demonstrated successful functionalization for both healthy and bleomycin-injured dECM.

wt% PEGαMA and 15% dECM, resulting in similar soft (4.9 ± 0.35) and stiffened (12.0 ± 0.58) mechanics that were not significantly different from the healthy hybrid-hydrogel formulation (Fig. 4c).

Fibroblast Activation

Fibroblasts were cultured on hybrid-hydrogels and assessed for expression of Col1a1 and αSMA promoters, characteristic of fibroblast activation,[13,41] *via* fluorescent microscopy. The percentage of cells expressing Col1a1 increased from 38.6 ± 3.1% on healthy, soft hydrogels to 77.8 ± 2.5% on healthy, stiffened hydrogels and from 40.4 ± 3.1% on bleo-

mycin-injured, soft hydrogels to 77 ± 2.6% on bleomycin-injured, stiffened hydrogels (Fig. 5b). Similarly, percentages of cells expressing αSMA increased with stiffening from 30.2 ± 2.6 to 76.5 ± 2.5% for healthy hybrid-hydrogels and from 32.0 ± 2.8 to 75.5 ± 2.7% for bleomycin-treated hybrid-hydrogels (Fig. 5b). Statistical differences were observed between soft and stiffened conditions ($p < 0.001$, 2-way ANOVA, Tukey Test); however, no statistical differences were evident between compositions. Additional analysis of the average intensity of each reporter per cell revealed that the healthy stiffened condition displayed an increase of 39.1% for Col1a1 and 46% for αSMA while the bleomycin-treated stiffened condition increased by 65.5% for Col1a1 and 75.9% for αSMA relative to the healthy soft condition (Fig. 5c). Statistical differences in average intensity per cell were measured between soft and stiffened ($p < 0.05$, 2-way ANOVA, Tukey Test), but not between healthy stiffened and bleomycin stiffened conditions ($p = 0.25$, 2-way ANOVA, Tukey Test). While no statistical differences were measured, a trend toward increasing intensity was observed when comparing bleomycin stiffened hydrogels to healthy stiffened hydrogels. Taken together, these data indicate the impact of substrate stiffness on fibroblast activation is greater than the influence of matrix composition on this hybrid-hydrogel platform.

DISCUSSION

Here, we describe engineering a model that enables researchers to decouple matrix mechanical properties from biochemical cues and explore cell-matrix interactions *in vitro*. Previous research from our group presented a strategy for incorporating healthy dECM into a dual-stage polymerizable hydrogel. These materials provided dynamic control over the extracellular mechanical environment and showed that stiffening increased activation of fibroblasts cultured on the hybrid-hydrogels.[29] In this manuscript, we build on that work by incorporating dECM derived from a murine model of bleomycin-induced pulmonary fibrosis to isolate and interrogate the effects of ECM composition as well as substrate mechanics (stiffness) on fibroblast activation. Findings from this study support that substrate stiffness induced significantly higher levels of fibroblast activation than biochemical changes in the dECM.

First, the efficacy of bleomycin injury and decellularization methodologies were confirmed. Bleomycin was administered as a single-dose intratracheal instillation 3 weeks prior to harvest, allowing for deposition and remodeling of the ECM.[37] A multi-dose regimen was not necessary for this study, because ECM ele-
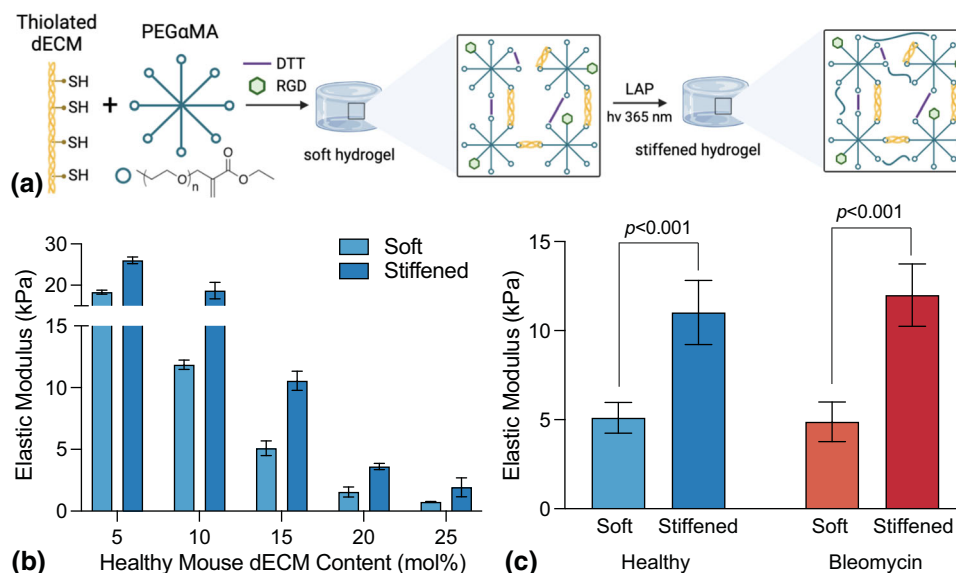
FIGURE 4. (a) Thiol-functionalized dECM, DTT, PEGαMA, and RGD were reacted through base-catalyzed Michael addition to form soft hydrogel. LAP incubation and exposure to UV light (365 nm) induced hydrogel stiffening. (b) Healthy dECM was incorporated into 18.5 wt% hydrogels at various dECM to DTT ratios ($N = 3$). (c) Elastic moduli of healthy and fibrotic dECM hybrid-hydrogel, before and after stiffening ($N = 9–10$).

ments were captured and processed prior to resolution of fibrosis.[31] Invasive lung function measurements[40] demonstrated that bleomycin had been correctly instilled and fibrosis-induced changes in lung mechanical function were achieved, reflected by decreased lung capacity (Fig. 1b) and quasi-static compliance (Fig. 1c). Furthermore, while a significant increase in lung elastance was found at PEEP = 9, elastance also trended higher at PEEP = 6, 3, and 0 (Fig. S3). A more prominent change in lung function at high airway pressures is not unexpected because the connective tissue network plays a more substantial role at higher lung volumes, while low-volume alveolar micromechanics are primarily governed by alveolar shape change, septal folding, and surfactant effects.[17] Taken together, these results indicated that stiffening due to fibrotic remodeling had occurred within bleomycin-injured lungs. Additionally, decellularization of both healthy and bleomycin-treated pulmonary tissue was confirmed following previously established criteria.[7] In accordance with Crapo et al., decellularized lungs were devoid of nuclear staining (Fig. 1d) and dsDNA fragments were below the threshold of 50 ng mg^{-1}, at 16.23 and 25.49 ng mg^{-1}, for healthy and bleomycin-injured, respectively (Fig. 1e).

Synthesizing hybrid-hydrogels containing dECM required that extracellular protein fragments be solubilized prior to functionalization. The relatively large ECM fragments obtained following decellularization remained poorly soluble even after robust mechanical digestion. Therefore, experiments were performed to determine a sufficient duration of enzymatic digestion

of dECM with pepsin to ensure solubility. Pepsin from porcine gastric mucosa has been used in the digestion of decellularized pulmonary tissue from human[8,42] and porcine[30] lungs, but has not been described for murine lung tissue. Digestion times varied from 24 to 72 h and significantly impacted solubility, protein fragmentation, and bulk mechanics of hydrogels made from these materials.[30] Here, dECM from healthy and bleomycin-injured mouse lungs was digested for 36 h. Protein concentration (Fig. 2a), amine content (Fig. 2b), and protein fragment size (Figs. 2c, 2d) were measured at 0, 4, 12, 24, and 36 h. Protein concentration plateaued after 4 h of enzymatic digestion for both healthy and bleomycin-injured dECM. However, free-amine content continued to increase up to 36 h of digestion, maximizing the potential amine-to-thiol conversion, and thus available functional moieties for crosslinking. Staining of dECM protein fragments separated by SDS-PAGE revealed relatively large protein fragments between 25 and 75 kDa remained, even following 36 h of pepsin digestion. Monomeric fibrillar collagens exhibit molecular weights between 250 and 300 kDa,[30,39] indicating that pepsin fragmented ECM collagens, but that these were not all further reduced in size with digestion time. Based on these results, 36 h duration of enzymatic pepsin digestion for both healthy and bleomycin-treated tissue was selected to maximize available protein concentration, free-amine content, and maintain consistent digestion protocols across dECM conditions.
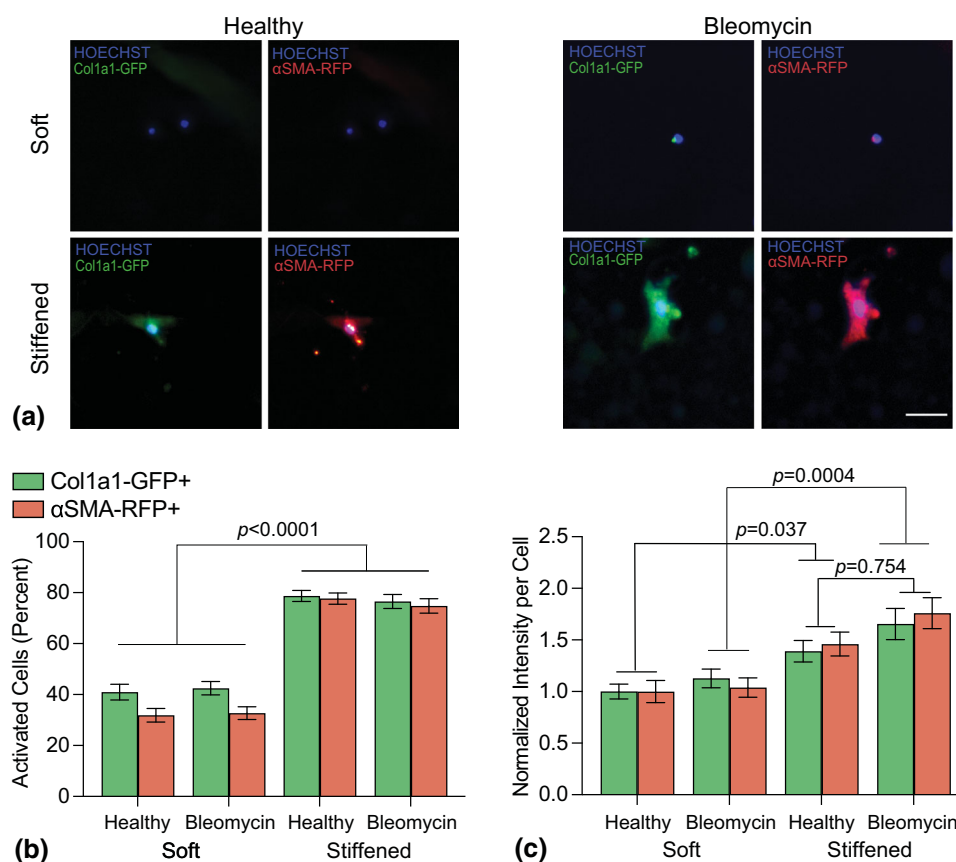
FIGURE 5. (a) Representative fluorescent images of fibroblasts cultured on hybrid-hydrogel showed expression of Col1a1 (Green) and αSMA (Red) promoters with a Hoechst nuclear counterstain (Blue). Scale bar, 25 μm. (b) Quantification of the percentage of fibroblasts expressing Col1a1 and αSMA of showed that microenvironmental stiffness significantly increased fibroblast activation ($p < 0.0001$, $N = 6$, 6 fields of view per image) while dECM origin did not. (c) Evaluating the average intensity of Col1a1 and αSMA expression per cell showed significant increases in expression on stiffened hybrid-hydrogels compared to soft controls ($p < 0.05$). While no statistical differences were measured, a trend toward increasing intensity was observed when comparing bleomycin stiffened hydrogels to healthy stiffened hydrogels ($p = 0.754$, $N = 6$, 6 fields of view per image).

Development of the hybrid-hydrogel formulation followed several distinct steps: (1) Identification of a sufficient amount of Traut's reagent to maximize thiolation of dECM amines; (2) Selection of the PE-GαMA weight percentage and DTT to dECM molar ratio necessary to emulate mechanics of healthy tissue during the initial base-catalyzed polymerization and fibrotic tissue following photoinitiated stiffening using healthy dECM; and (3) replication of the hybrid-hydrogel formulation with bleomycin-injured dECM. Residual amine content was minimized after thiolation with a 75-molar excess of Traut's reagent (Fig. 3a). Moreover, thiol concentrations post-thiolation were observed to be between 0.10 and 0.3 μmol mg^{-1} (Fig. 3b), aligning with previous studies in which thiol concentration of thiolated porcine lung was observed to be about 0.2 μmol mg^{-1}.[29] After thiolation, 18.5 wt% PEGαMA was chosen to bring the initial hydrogel elastic modulus within range of healthy lung stiffness (1–5 kPa), while several dECM to DTT ratios

were evaluated to enable photoinitiated stiffening to fibrotic levels (> 10 kPa) (Fig. 4b).[8,19,21] A final hybrid-hydrogel formulation containing 15% dECM with 85% DTT resulted in modulus values that met these criteria in the soft (5.11 ± 0.86 kPa) and stiffened states (11.02 ± 1.80 kPa).

Previous studies have linked the combination of biochemical and biomechanical alterations that occur in the ECM during pulmonary fibrosis to fibroblast activation. Schiller et al. performed time-resolved proteomic analysis of bleomycin-injured mouse lungs to characterize changes associated with inflammation (day 3), fibrogenesis (day 14), remodeling (day 28), and resolution (day 54).[37] Over 3000 proteins, including 154 matrisome components, changed significantly across this study. For instance, the ECM glycoprotein tenascin-C increased during fibrogenesis and was associated with stiffer lung tissue.[37] Typically, α3- and α5-laminins are the most abundant in adult mouse lung tissue. At days 3 and 14 after injury, this abundance

was downregulated accompanied by an upregulation of collage type IV.[37] There were also notable changes in 365 known targets of transforming growth factor β (TGF-β) signaling indicating this key regulator of fibrogenesis was highly upregulated at day 14 after injury.[37] Booth *et al.* used decellularized human precision-cut lung slices from healthy and IPF human lungs as cell culture platforms and showed that fibrotic matrices promoted fibroblast activation as measured by increases in αSMA production.[5] Similarly, Parker *et al.* cultured healthy and IPF fibroblasts on decellularized human precision-cut lung slices from healthy and IPF human lungs and found that dECM origin was a stronger regulator of fibroblast activation than cell origin.[28] Other studies have investigated the influence of increased microenvironmental stiffness alone on fibroblast activation in the context of pulmonary fibrosis and found a positive correlation between substrate stiffness and activation on static surfaces.[2,20] Petrou *et al.* cultured primary murine fibroblasts on soft (3.63 ± 0.24 kPa) and dynamically stiffened (13.35 ± 0.83 kPa) hybrid-hydrogels containing healthy dECM, observing a greater than twofold increase in proportion of cells expressing Col1a1 and αSMA, proving similar fibroblast activation results can be achieved through dynamic changes in substrate mechanics.[29]

The phototunable hybrid-hydrogel detailed in this report is a platform that enables the investigation of cellular responses to matrix composition and dynamic changes in mechanical properties in a way that decouples microenvironmental mechanics from composition. Sava *et al.* have reported one of the only other biomaterial platforms designed to decouple these properties that are intrinsically linked *in vivo*. Polyacrylamide hydrogels designed to mimic healthy (1.8 ± 0.5 kPa) and fibrotic (23.7 ± 2.3 kPa) lung tissue were coated with healthy or IPF-derived lung dECM. Cells cultured on the high-stiffness hydrogels exhibited significantly increased cell area, elongation, and expression of αSMA compared to soft substrates independent of dECM origin.[36] In the current report, PDGFRα+ fibroblasts from dual-reporter mice were cultured on the surface of hybrid-hydrogels to evaluate fibroblast activation in response to differences in composition and dynamic stiffening. Fibroblasts cultured on stiffened hydrogels displayed a twofold increase in the percentage of cells expressing Col1a1 or αSMA, while composition of the dECM (healthy versus bleomycin-treated) did not significantly impact the percentage of fibroblasts expressing Col1a1 and αSMA (Fig. 5b), similar to results reported by Sava *et al.* Interestingly, intensity measurements of Col1a1 and αSMA expression trended upwards between healthy and bleomycin stiffened conditions. There was a nearly 20% increase in average intensity per cell between these hydrogel conditions, indicating composition may be a contributing, but less significant driver of fibroblast activation.

CONCLUSIONS

Phototunable hybrid-hydrogels were engineered to decouple the dependence of substrate mechanics from the biochemical composition of the matrix and then used to investigate activation of fibroblasts isolated from dual-transgenic Col1a1-GFP and αSMA-RFP reporter mice. It was observed that substrate stiffness significantly impacted fibroblast activation and the intensity of Col1a1-GFP and αSMA-RFP expression trended upwards with a diseased dECM composition. Taken together, this evidence supports that substrate stiffness is the primary, but not sole contributor to fibrotic activation. Moreover, the incorporation of healthy and diseased dECM into a phototunable hybrid-hydrogel as the crosslinker enables the encapsulation and study of fibroblast responses to independent changes in matrix composition and mechanical properties in 3D, an advance that allows future experiments to improve our understanding of the cellular and molecular drivers of pulmonary fibrosis.

SUPPLEMENTARY INFORMATION

The online version contains supplementary material available at https://doi.org/10.1007/s12195-022-00726-y.

ACKNOWLEDGMENTS

AUTHOR CONTRIBUTIONS

KSS, RH, PS, RB, BJS, DWHR, and CMM conceived the research plan. KSS, RH, PS, RB, BJS, SEN,

and BE carried out experiments. All authors wrote, reviewed, and edited the manuscript.

DATA AVAILABILITY

CONFLICT OF INTEREST

Dr. Magin is an inventor on a pending patent related to the technology described in this manuscript. All remaining authors (KSS, RH, PS, RB, BJS, SEN, BE, and DWHR) have no conflicts of interest to disclose.

HUMAN STUDIES

No human studies were carried out by the authors for this article.

ANIMAL STUDIES

All institutional and national guidelines for the care and use of laboratory animals were followed and approved by the appropriate institutional committees.

REFERENCES

[1]Arkenberg, M. R., H. D. Nguyen, and C. C. Lin. Recent advances in bio-orthogonal and dynamic crosslinking of biomimetic hydrogels. *J. Mater. Chem. B*. 8:7835–7855, 2020.

[2]Balestrini, J. L., S. Chaudhry, V. Sarrazy, A. Koehler, and B. Hinz. The mechanical memory of lung myofibroblasts. *Integr. Biol. (Camb)*. 4:410–421, 2012.

[3]Barbarin, V., A. Nihoul, P. Misson, M. Arras, M. Delos, I. Leclercq, D. Lison, and F. Huaux. The role of pro- and anti-inflammatory responses in silica-induced lung fibrosis. *Respir. Res*. 6:112, 2005.

[4]Bolukbas, D. A., M. M. De Santis, H. N. Alsafadi, A. Doryab, and D. E. Wagner. The preparation of decellularized mouse lung matrix scaffolds for analysis of lung regenerative cell potential. *Methods Mol. Biol*. 275–295:2019, 1940.

[5]Booth, A. J., R. Hadley, A. M. Cornett, A. A. Dreffs, S. A. Matthes, J. L. Tsui, K. Weiss, J. C. Horowitz, V. F. Fiore, T. H. Barker, B. B. Moore, F. J. Martinez, L. E. Niklason,

and E. S. White. Acellular normal and fibrotic human lung matrices as a culture system for *in vitro* investigation. *Am. J. Respir. Crit. Care Med*. 186:866–876, 2012.

[6]Christensen, P. J., R. E. Goodman, L. Pastoriza, B. Moore, and G. B. Toews. Induction of lung fibrosis in the mouse by intratracheal instillation of fluorescein isothiocyanate is not T-cell-dependent. *Am. J. Pathol*. 155:1773–1779, 1999.

[7]Crapo, P. M., T. W. Gilbert, and S. F. Badylak. An overview of tissue and whole organ decellularization processes. *Biomaterials*. 32:3233–3243, 2011.

[8]de Hilster, R. H. J., P. K. Sharma, M. R. Jonker, E. S. White, E. A. Gercama, M. Roobeek, W. Timens, M. C. Harmsen, M. N. Hylkema, and J. K. Burgess. Human lung extracellular matrix hydrogels resemble the stiffness and viscoelasticity of native lung tissue. *Am. J. Physiol. Lung Cell. Mol. Physiol*. 318:L698–L704, 2020.

[9]DellaLatta, V., A. Cecchettini, S. DelRy, and M. A. Morales. Bleomycin in the setting of lung fibrosis induction: from biological mechanisms to counteractions. *Pharmacol. Res*. 97:122–130, 2015.

[10]Dolhnikoff, M., T. Mauad, and M. S. Ludwig. Extracellular matrix and oscillatory mechanics of rat lung parenchyma in bleomycin-induced fibrosis. *Am. J. Respir. Crit. Care Med*. 160:1750–1757, 1999.

[11]Gillette, B. M., J. A. Jensen, M. Wang, J. Tchao, and S. K. Sia. Dynamic hydrogels: switching of 3D microenvironments using two-component naturally derived extracellular matrices. *Adv. Mater*. 22:686–691, 2010.

[12]Haak, A. J., Q. Tan, and D. J. Tschumperlin. Matrix biomechanics and dynamics in pulmonary fibrosis. *Matrix Biol*. 73:64–76, 2018.

[13]Heinzelmann, K., M. Lehmann, M. Gerckens, N. Noskovicova, M. Frankenberger, M. Lindner, R. Hatz, J. Behr, A. Hilgendorff, M. Konigshoff, and O. Eickelberg. Cell-surface phenotyping identifies CD36 and CD97 as novel markers of fibroblast quiescence in lung fibrosis. *Am. J. Physiol. Lung Cell. Mol.r Physiol*. 315:L682–L696, 2018.

[14]Herrera, J., C. A. Henke, and P. B. Bitterman. Extracellular matrix as a driver of progressive fibrosis. *J. Clin. Invest*. 128:45–53, 2018.

[15]Jones, M. G., A. Fabre, P. Schneider, F. Cinetto, G. Sgalla, M. Mavrogordato, S. Jogai, A. Alzetani, B. G. Marshall, K. M. O'Reilly, J. A. Warner, P. M. Lackie, D. E. Davies, D. M. Hansell, A. G. Nicholson, I. Sinclair, K. K. Brown, and L. Richeldi. Three-dimensional characterization of fibroblast foci in idiopathic pulmonary fibrosis. *JCI Insight*. 2016. https://doi.org/10.1172/jci.insight.86375.

[16]Keith, R. C., J. L. Powers, E. F. Redente, A. Sergew, R. J. Martin, A. Gizinski, V. M. Holers, S. Sakaguchi, and D. W. Riches. A novel model of rheumatoid arthritis-associated interstitial lung disease in SKG mice. *Exp. Lung Res*. 38:55–66, 2012.

[17]Knudsen, L., E. Lopez-Rodriguez, L. Berndt, L. Steffen, C. Ruppert, J. H. T. Bates, M. Ochs, and B. J. Smith. Alveolar micromechanics in bleomycin-induced lung injury. *Am. J. Respir. Cell Mol. Biol*. 59:757–769, 2018.

[18]Korfei, M., S. Schmitt, C. Ruppert, I. Henneke, P. Markart, B. Loeh, P. Mahavadi, M. Wygrecka, W. Klepetko, L. Fink, P. Bonniaud, K. T. Preissner, G. Lochnit, L. Schaefer, W. Seeger, and A. Guenther. Comparative proteomic analysis of lung tissue from patients with idiopathic pulmonary fibrosis (IPF) and lung transplant donor lungs. *J. Proteome Res*. 10:2185–2205, 2011.

[19]Liu, F., C. M. Haeger, P. B. Dieffenbach, D. Sicard, I. Chrobak, A. M. F. Coronata, M. M. S. Velandia, S. Vitali, R. A. Colas, P. C. Norris, S. A. Marinkovic, X. L. Liu, J. Ma, C. D. Rose, S. J. Lee, S. A. A. Comhair, S. C. Erzurum, J. D. McDonald, C. N. Serhan, S. R. Walsh, D. J. Tschumperlin, and L. E. Fredenburgh. Distal vessel stiffening is an early and pivotal mechanobiological regulator of vascular remodeling and pulmonary hypertension. *JCI Insight*. 2016. https://doi.org/10.1172/jci.insight.86987.

[20]Liu, F., D. Lagares, K. M. Choi, L. Stopfer, A. Marinkovic, V. Vrbanac, C. K. Probst, S. E. Hiemer, T. H. Sisson, J. C. Horowitz, I. O. Rosas, L. E. Fredenburgh, C. Feghali-Bostwick, X. Varelas, A. M. Tager, and D. J. Tschumperlin. Mechanosignaling through YAP and TAZ drives fibroblast activation and fibrosis. *Am. J. Physiol. Lung Cell. Mol. Physiol*. 308:L344–L357, 2015.

[21]Liu, F., and D. J. Tschumperlin. Micro-mechanical characterization of lung tissue using atomic force microscopy. *J. Vis. Exp*. 2011. https://doi.org/10.3791/2911.

[22]Liu, S. S., C. Liu, X. X. Lv, B. Cui, J. Yan, Y. X. Li, K. Li, F. Hua, X. W. Zhang, J. J. Yu, J. M. Yu, F. Wang, S. Shang, P. P. Li, Z. G. Zhou, Y. Xiao, and Z. W. Hu. The chemokine CCL1 triggers an AMFR-SPRY1 pathway that promotes differentiation of lung fibroblasts into myofibroblasts and drives pulmonary fibrosis. *Immunity*. 54:2433–2435, 2021.

[23]Manali, E. D., C. Moschos, C. Triantafillidou, A. Kotanidou, I. Psallidas, S. P. Karabela, C. Roussos, S. Papiris, A. Armaganidis, G. T. Stathopoulos, and N. A. Maniatis. Static and dynamic mechanics of the murine lung after intratracheal bleomycin. *BMC Pulm. Med*. 11:33, 2011.

[24]Meyvis, T. K. L., S. C. De Smedt, J. Demeester, and W. E. Hennink. Rheological monitoring of long-term degrading polymer hydrogels. *J. Rheol*. 43:933–950, 1999.

[25]Moore, B. B., and C. M. Hogaboam. Murine models of pulmonary fibrosis. *Am. J. Physiol. Lung Cell. Mol. Physiol*. 294:L152-160, 2008.

[26]National Research Council (U.S.). Committee for the update of the guide for the care and use of laboratory animals, Institute for Laboratory Animal Research (U.S.) and National Academies Press (U.S.). Guide for the care and use of laboratory animals. Washington, D.C.: National Academies Press, 2011, p. xxv, 220 p.

[27]Nizamoglu, M., R. H. J. de Hilster, F. Zhao, P. K. Sharma, T. Borghuis, O. M. C. Harmsen, and J. K. Burgess. An *in vitro* model of fibrosis using crosslinked native extracellular matrix-derived hydrogels to modulate biomechanics without changing composition. *bioRxiv*. 2022. https://doi.org/10.1101/2022.02.02.478812.

[28]Parker, M. W., D. Rossi, M. Peterson, K. Smith, K. Sikstrom, E. S. White, J. E. Connett, C. A. Henke, O. Larsson, and P. B. Bitterman. Fibrotic extracellular matrix activates a profibrotic positive feedback loop. *J. Clin. Investig*. 124:1622–1635, 2014.

[29]Petrou, C. L., T. J. D'Ovidio, D. A. Bolukbas, S. Tas, R. D. Brown, A. Allawzi, S. Lindstedt, E. Nozik-Grayck, K. R. Stenmark, D. E. Wagner, and C. M. Magin. Clickable decellularized extracellular matrix as a new tool for building hybrid-hydrogels to model chronic fibrotic diseases *in vitro*. *J. Mater. Chem. B*. 8:6814–6826, 2020.

[30]Pouliot, R. A., P. A. Link, N. S. Mikhaiel, M. B. Schneck, M. S. Valentine, F. J. Kamga Gninzeko, J. A. Herbert, M. Sakagami, and R. L. Heise. Development and characterization of a naturally derived lung extracellular matrix hydrogel. *J. Biomed. Mater. Res. A*. 104:1922–1935, 2016.

[31]Redente, E. F., B. P. Black, D. S. Backos, A. N. Bahadur, S. M. Humphries, D. A. Lynch, R. M. Tuder, R. L. Zemans, and D. W. H. Riches. Persistent, progressive pulmonary fibrosis and epithelial remodeling in mice. *Am. J. Respir. Cell. Mol. Biol*. 64:669–676, 2021.

[32]Richeldi, L., H. R. Collard, and M. G. Jones. Idiopathic pulmonary fibrosis. *Lancet*. 389:1941–1952, 2017.

[33]Rosales, A. M., S. L. Vega, F. W. DelRio, J. A. Burdick, and K. S. Anseth. Hydrogels with reversible mechanics to probe dynamic cell microenvironments. *Angew. Chem. Int. Ed. Engl*. 56:12132–12136, 2017.

[34]Rube, C. E., D. Uthe, K. W. Schmid, K. D. Richter, J. Wessel, A. Schuck, N. Willich, and C. Rube. Dose-dependent induction of transforming growth factor beta (TGF-beta) in the lung tissue of fibrosis-prone mice after thoracic irradiation. *Int. J. Radiat. Oncol. Biol. Phys*. 47:1033–1042, 2000.

[35]Saldin, L. T., M. C. Cramer, S. S. Velankar, L. J. White, and S. F. Badylak. Extracellular matrix hydrogels from decellularized tissues: structure and function. *Acta Biomater*. 49:1–15, 2017.

[36]Sava, P., A. Ramanathan, A. Dobronyi, X. Peng, H. Sun, A. Ledesma-Mendoza, E. L. Herzog, and A. L. Gonzalez. Human pericytes adopt myofibroblast properties in the microenvironment of the IPF lung. *JCI Insight*. 2:e96352, 2017.

[37]Schiller, H. B., I. E. Fernandez, G. Burgstaller, C. Schaab, R. A. Scheltema, T. Schwarzmayr, T. M. Strom, O. Eickelberg, and M. Mann. Time- and compartment-resolved proteome profiling of the extracellular niche in lung injury and repair. *Mol. Syst. Biol*. 11:819, 2015.

[38]Shi, X., Y. Chen, Q. Liu, X. Mei, J. Liu, Y. Tang, R. Luo, D. Sun, Y. Ma, W. Wu, Y. Tu, Y. Zhao, W. Xu, Y. Ke, S. Jiang, Y. Huang, R. Zhang, L. Wang, Y. Chen, J. Xia, W. Pu, H. Zhu, X. Zuo, Y. Li, J. Xu, F. Gao, D. Wei, J. Chen, W. Yin, Q. Wang, H. Dai, L. Yang, G. Guo, J. Cui, N. Song, H. Zou, S. Zhao, J. H. W. Distler, L. Jin, and J. Wang. LDLR dysfunction induces LDL accumulation and promotes pulmonary fibrosis. *Clin. Transl. Med*.12:e711, 2022.

[39]Silver, F. H., and D. E. Birk. Molecular-structure of collagen in solution—comparison of type-I, type-Ii, type-Iii and type-V. *Int. J. Biol. Macromol*. 6:125–132, 1984.

[40]Smith, B. J., G. S. Roy, A. Cleveland, C. Mattson, K. Okamura, C. M. Charlebois, K. L. Hamlington, M. V. Novotny, L. Knudsen, M. Ochs, R. D. Hite, and J. H. T. Bates. Three alveolar phenotypes govern lung function in murine ventilator-induced lung injury. *Front. Physiol*. 11:660, 2020.

[41]Tsukui, T., K. H. Sun, J. B. Wetter, J. R. Wilson-Kanamori, L. A. Hazelwood, N. C. Henderson, T. S. Adams, J. C. Schupp, S. D. Poli, I. O. Rosas, N. Kaminski, M. A. Matthay, P. J. Wolters, and D. Sheppard. Collagen-producing lung cell atlas identifies multiple subsets with distinct localization and relevance to fibrosis. *Nat. Commun*. 11:1920, 2020.

[42]Wagner, D. E., N. R. Bonenfant, D. Sokocevic, M. J. DeSarno, Z. D. Borg, C. S. Parsons, E. M. Brooks, J. J. Platz, Z. I. Khalpey, D. M. Hoganson, B. Deng, Y. W. Lam, R. A. Oldinski, T. Ashikaga, and D. J. Weiss. Three-dimensional scaffolds of acellular human and porcine lungs for high throughput studies of lung disease and regeneration. *Biomaterials*. 35:2664–2679, 2014.

[43]Wang, Y., L. Zhang, T. Huang, G. R. Wu, Q. Zhou, F. X. Wang, L. M. Chen, F. Sun, Y. Lv, F. Xiong, S. Zhang, Q.

Yu, P. Yang, W. Gu, Y. Xu, J. Zhao, H. Zhang, W. Xiong, and C. Y. Wang. The methyl-CpG-binding domain 2 facilitates pulmonary fibrosis by orchestrating fibroblast to myofibroblast differentiation. *Eur. Respir. J.* 2022. https://doi.org/10.1183/13993003.03697-2020.

[44]Wolters, P. J., H. R. Collard, and K. D. Jones. Pathogenesis of idiopathic pulmonary fibrosis. *Annu. Rev. Pathol.* 9:157–179, 2014.

[45]Wu, S. M., J. J. Tsai, H. C. Pan, J. L. Arbiser, L. Elia, and M. L. Sheu. Aggravation of pulmonary fibrosis after knocking down the aryl hydrocarbon receptor in the insulin-like growth factor 1 receptor pathway. *Br. J. Pharmacol.* 179:3430–3451, 2022.

[46]Zhang, Y., M. Jiang, M. Nouraie, M. G. Roth, T. Tabib, S. Winters, X. Chen, J. Sembrat, Y. Chu, N. Cardenes, R. M. Tuder, E. L. Herzog, C. Ryu, M. Rojas, R. Lafyatis, K. F. Gibson, J. F. McDyer, D. J. Kass, and J. K. Alder. GDF15 is an epithelial-derived biomarker of idiopathic pulmonary fibrosis. *Am. J. Physiol. Lung Cell. Mol. Physiol.* 317:L510–L521, 2019.